IJES *Iranian Journal of Earth Sciences*
Vol. 13, No. 1, 2021, 31-40.

Prognosis of of gold mineralization phases by multifractal modeling in the Zehabad epithermal deposit, NW Iran

Somaye Shahbazi [1], Majid Ghaderi*[1], Peyman Afzal [2]

1. Department of Economic Geology, Tarbiat Modares University, Tehran, Iran
2 Department of Mining Engineering, South Tehran Branch, Islamic Azad University, Tehran, Iran

Received 7 December 2018; accepted 21 October 2019

Abstract

Concentration–Number (C–N) fractal method has been used for determining and separating mineralization phases based on surface lithogeochemical Au, Ag, Cu, Pb, Zn, As and Sb data in the Zehabad epithermal deposit, NW Iran. Five mineralization phases are demonstrated by multifractal modeling for the mentioned elements correlating with geological studies. The extreme phase of Au mineralization is higher than 7.9 ppm, which is correlated with hematite deposition in silicic veins and veinlets, whereas Ag (>79.43 ppm), Cu (>15.85%), Pb (>63.1%), Zn (>11.2%) extreme phases are associated with the main stage sulfidation phases. The results show that Au, Cu, Pb, Zn and Ag have two different mineralization trends based on the multifractal nature in this area. These trends are presented based on oxidic and sulfidic mineralization. According to mineralogical studies, the main stages of mineralization include: 1) formation of chalcopyrite ± sphalerite in silicic veins in sulfidic trend; 2) deposition of native gold and specular hematite in silicic veins in response to boilling, in oxidic trend; 3) next phase of fluid penetration and replacing chalcopyrite by galena, sphalerite and tetrahedrite-tennantite in the sulfide veins, in sulfic trend. Neighbouring copper and silver are due to the formation of tetrahedrite-tennantite solid solution. The obtained results show a positive correlation between mineralization phases and the faults present at the deposit. Moreover, mineralization phases of these elements demonstrate a good correlation with silicification and silicic veins and veinlets.

Keywords: *Gold mineralization phases, Concentration-Number (C–N) fractal method, epithermal, Zehabad*

1. Introduction

Determination of mineralization phases is important for mineral exploration especially prediction of ore deposition in a studied area. Different experimental and mathematical methods have been proposed for this purpose based on geological and mineralographical characteristics

Mathematical modeling is used for different branches of geosciences one of which is fractal/multifractal modeling utilized for separation of different anomalies and mineralized zones (e.g., Cheng et al. 1994; Agterberg 1996 ; Sim et al. 1999; Li et al. 2003; Afzal et al. 2011; 2013, 2017; Khalili and Afzal 2018). Various fractal methods suggested for this type of studies include Concentration-Area (C-A; Cheng et al. 1994), Concentration-Volume (C-V; Afzal et al. 2011) and Concentration-Number (C-N; Hassanpour and Afzal 2013). These methods are based on the power law relationship between studied attributes (elemental grades in this scenario) and occupied geometrical properties such as area, perimeter and volume of these attributes. For example, there is a power law equation between elemental concentrations and cumulative number of geochemical samples.

Zehabad epithermal deposit is located in 57 km NW of the city of Qazvin in the Tarom-Hashtjin subzone of Alborz structural zone, NW Iran (Fig 1). The Tarom subzone includes several epithermal deposits such as Aliabad-Khanchi (Kouhestani et al. 2018), Chodarchay (Yasami et al. 2018), Goloujeh (Mehrabi et al. 2016) and Khalifelou (Esmaeli et al. 2015). These deposits are hosted by Eocene volcanic and volcano-sedimentary sequences and were under the influence of the upper Eocene intrusive bodies. In addition, there are many Iron Oxide – Apatite (IOA) deposits in the region (Nabatian and Ghaderi 2014; Nabatian et al. 2014; Mokhtari et al. 2018). Both types of mineralization are related to the monzodiorite porphyry intrusions (Castro et al. 2013).

German miners explored gold, silver, lead and zinc minerals at the Zehabad deposit from 1951 to 1977 (Amin Khorramdasht Exploration Company, 2006). Detailed exploration is currently carried out by lithogeochemical exploration from surface as well as from tunnels and core drilling (Shahbazi et al. 2019). Most of mineralized veins formed in tuffs in this deposit. Base and precious metals mineralization is association with quartz and quartz-carbonate veins, parallel to both fracture systems. Moreover, andesite-dacite lavas and microdiorite porphyry intrusion host several ore-bearing veins and in the NE and western parts of the studied area (Shahbazi and Ghaderi 2014).According to microscopic studies and systematic geochemical sampling in the area, mineralization is related to quartz-sulfide and quartz-carbonate-sulfide veins and their altered wall rocks (Shahbazi et al. 2019). Native gold particles are visible in a few samples.

---

*Corresponding author.
E-mail address (es): mghaderi@modares.ac.ir

The aim of this study is to determine Au, Ag, Pb, Zn, Cu, As and Sb mineralization phases using C-N multifractal modeling at the Zehabad epithermal deposit. In addition, the results obtained by this fractal modeling is compared with various geological lines of evidence especially ore microscopic data.

2. Geological setting

2.1. Regional geology

The Zehabad deposit is situated in the Alborz-Azerbaijan sedimentary-structural zone (Nabavi 1976). Western part of the Alborz Mountains are divided to several subzones in trend of NE-SW which are Talesh, Ghezelozan, Tarom and Ardin. This deposit is located in the Tarom subzone (Fig 1). The Eocene extensive phase caused deposition of Karaj sedimentary-volcanic Formation in shallow environment (Asiabanha and Foden 2012). However, study by Asiabanha and Foden (2012) shows that the intrusive units with Eocene and later ages have a genetic relation with volcanic part of the Karaj Formation. The intrusions have a composition variation between dioritic to monzonitic and syenitic types (Aghazadeh et al., 2011; Castro et al., 2013). In addition, age of these intrusive rocks are determined to upper Eocene based on Rezaeian et al. (2012) and Nabatian et al. (2017) studies. This deposit is located between to two strike slip thrusts which are Manjil and Zanjan faults in the northern and southern borders, respectively. These faults occurred proper approaches for ore forming fluids of different ore deposits' types in the studied area at Cenozoic.

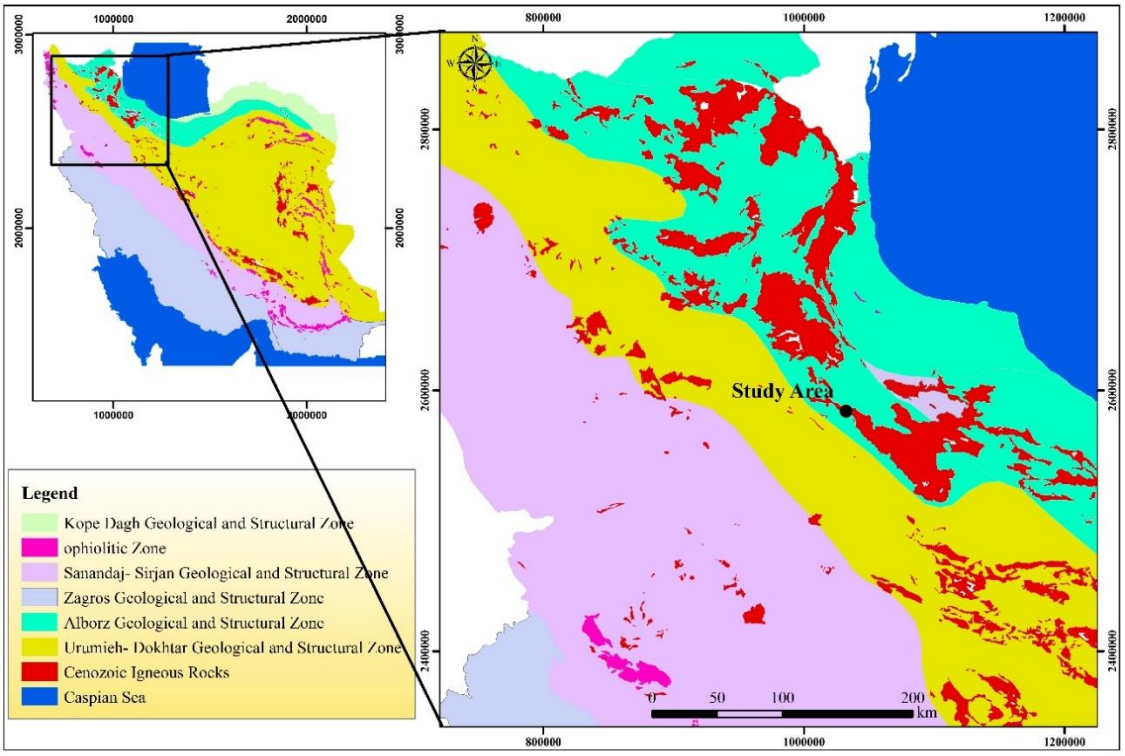

Fig 1. Location of the study area in the Iranian structural zones (Modified after Sahandi et al. 1985).

2.2. Geology of the Zehabad deposit

Eocene volcanic and volcano sedimentary rocks in Zehabad area formed intermediate to acidic composition, including porphyritic rhyolite, andesite, latite, dacite to quartz trachyte and laminations of tuffaceous shale to sandy tuffs (Fig 2). Intrusive bodies consist of microdiorite and monzonite/quartz monzonite porphyry as stock and dyke which inject in upper Eocene and hosted by volcanic and volcano-sedimentary units. All of outcrops cut by the NW-SE, and also; Quaternary units were intersected by the NE-SW faults and fractures.

According to systematic drilling and tunnel sampling, the ore proved reserves at western veins of the Zehabad deposit is 150,000 tons with summation of Pb and Zn about 7.7%. Furthermore, there are 8 ppm Au and 600 ppm Ag due to the concentration of galena in mineral processing plant (Shahbazi et al. 2018).

2.3. Alteration

Hydrothermal alteration zones at the Zehabad deposit mainly include silicification surrounded by widespread argillic alteration. In some places, the argillic zone locally changes to thin bands of propylitic alteration contain chlorite and epidote (Fig 3).

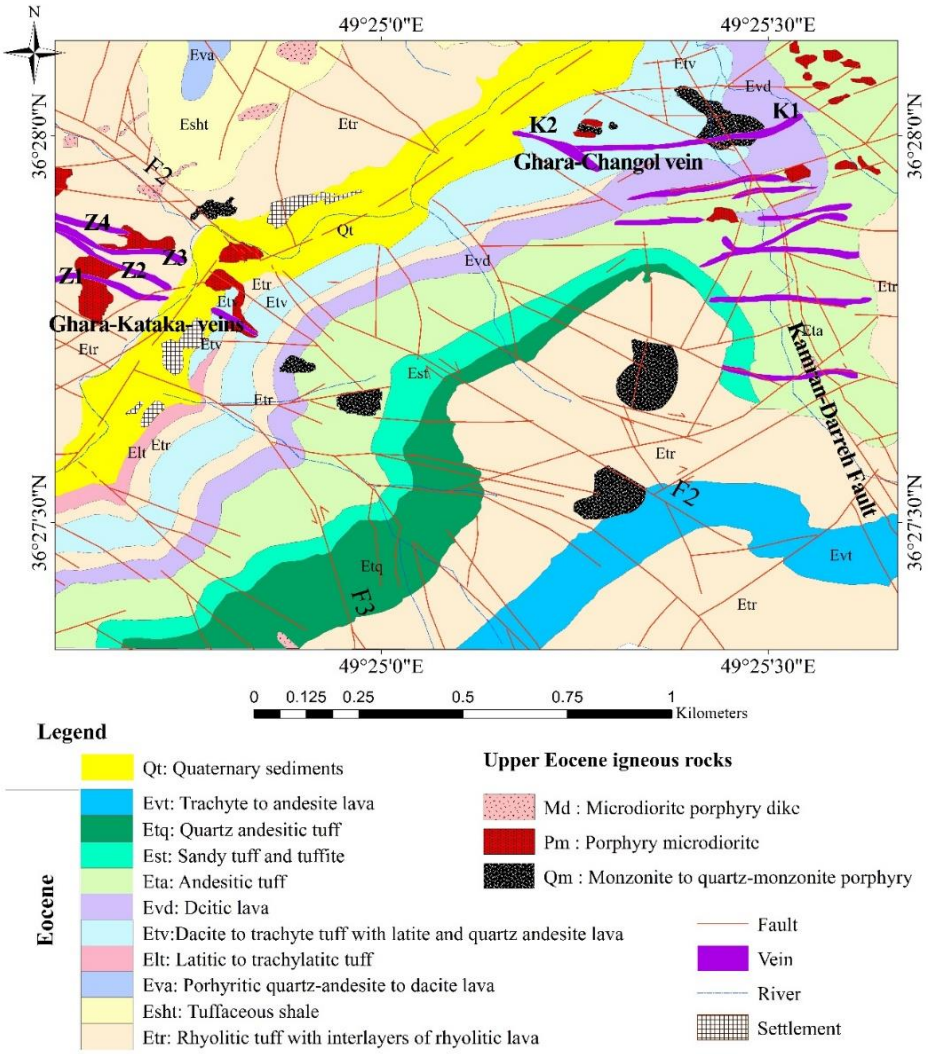

Fig 2. Geological map of the Zehabad deposit (Shahbazi et al. 2019).

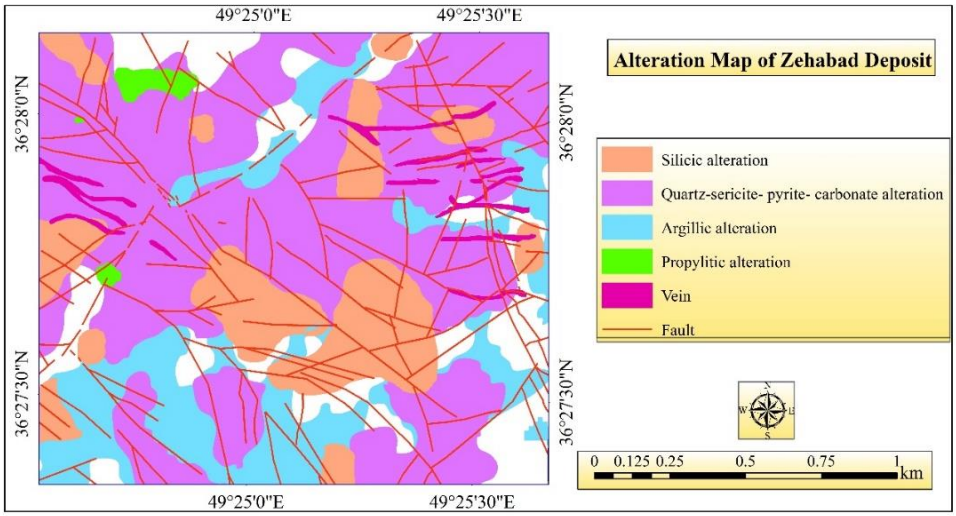

Fig 3. Alteration map of the Zehabad deposit (Shahbazi 2020).

The argillic zone consists of kaolinite, illite, smectite and montmorillonite. Sericitization is extended in the studied area especially covering intrusions with pyrite, quartz and calcite. Finally, silica sinter covered these sequences, remaining only a few pieces of this sinter on the slopes. The silicification is the inner part of this alteration system which contains base and precious metals. This type of alteration and followed mineralization were controlled by fault and fracture systems (Shahbazi et al. 2019).

2.4. Mineralization

Ore-bearing breccia veins at the Zehabad deposit formed during five stages. In all stages mineralization occurred as cement of breccia. Firstly, pyrite, chalcopyrite and sphalerite were produced as amorphous sulfidic gels with very low grade and extension (Fig 4A). In the second stage, euhedral to subhedral pyrite, chalcopyrite and sphalerite surrounded Prior sulfidic gels (Fig 4A).

The third stage includes deposition of quartz and specular hematite in response to boilling. Thus, native gold particles with specularite/hematite formed due to this phenomena (Fig 4E). The fourth stage represents as replacement of the first and second stages ore minerals by galena, sphalerite, tennantite-tetrahedrite and pyrite (Fig 4B). Native gold precipitates as inclusion in galena and sphalerite in this stage (Fig 4C & D). Introduction of silicic-carbonate fluids brecciated the sulfide veins in the fifth stage (Fig 4F).

3. Methodology

The Number-Size (N-S) was introduced by Mandelbrot (1983) for classification of different phenomena such as islands, trees and geological features (Mandelbrot, 1983; Turcotte, 1997). Agterberg (1995) developed this method for categorizing Cu-Au deposits in Quebec and Ontario, Canada. Hassanpour and Afzal (2013) proposed the C-N model for separation of geochemical anomalies in the Haftcheshmeh porphyry system. This method is proposed based on reverse relationship between ore grade and occupied samples as following form:

$N (\geq \rho) \propto \rho - \beta$ (1)

where N ($\geq \rho$) shows the sample number with concentration values greater than the ρ value. ρ is the concentration of element and β is the fractal dimension. In this method, geochemical data has not undergone pre-treatment and estimation.

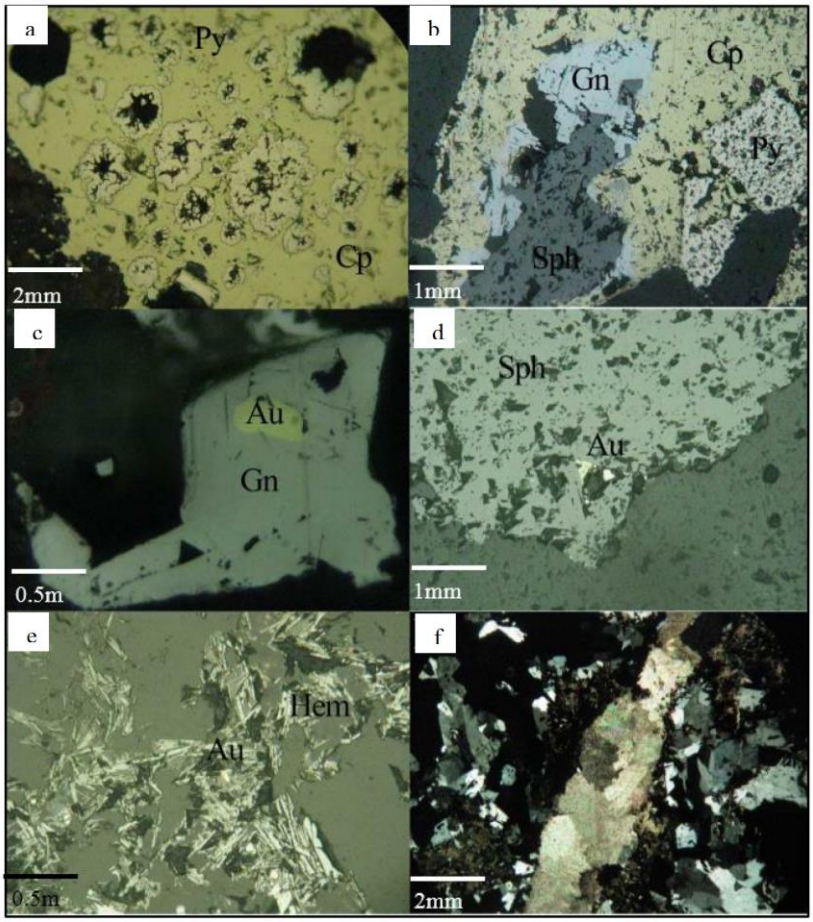

Fig 4. Mineralization stages. a: Stage I pyrite surrounded by chalcopyrite of stage II. b) Stage II minerals (pyrite and chalcopyrite) replaced by stage IV (galena and sphalerite). c) Inclusion of native gold in galena. d) Inclusion of native gold in sphalerite. e) Formation of gold and hematite in stage III. f) Quartz-carbonate vein cut all mineralization phases.

In this study, the results of the C-N fractal modeling were correlated and compared with the geological parameters including mineralographical, geological evidences and alteration features. Consequently, gold mineralization phases were defined by results derived via the C-N fractal modeling and geological characteristics.

4. Dataset

A total of 384 rock samples were collected from silicic veins and were analysed by Fire assay, ICP-OES and ICP-MS at Acme laboratory in Canada. These analyses were carried out for 42 elements including Pb, Zn, Ag and Au. Detection limits for Au, Cu, Pb, Zn and Ag are 1 ppb, 0.2 ppm, 0.2 ppm, 0.2 ppm and 0.01 ppm, respectively.

5. Discussion

In this paper, the C-N log-log plots were obtained for Au, As, Sb, Ag, Cu, Pb and Zn (Fig 5). There are six geochemical populations for Au, Ag, Cu, Pb and Zn. In addition, five and four populations were separated for As and Sb, respectively, as depicted in Fig. 5. Elemental log-log plots indicate a multifractal nature for these elements based on more than two populations and bench shape which can show different phases of mineralization. The main section for Au mineralization started from 2.24 ppm, while major mineralization for Ag, Cu, Pb and Zn commenced from 8 ppm, 0.1259 %, 0.63% and 0.6309 %, respectively. Gold highly and enriched mineralized veins started from 2.238 ppm and 7.943 ppm, respectively. Fractal dimensions (FDs) for main population of mineralization for these elements are higher than 0.6 and enriched zones have FDs more than 1. In addition, the FDs for elemental background are lower than 0.15, as depicted in Fig. 5.

The main mineralized veins (highly and enriched) include K1, K2, Z1, Z2 and Z3 which are located in the NE and SW parts of the area (Fig 6). These are associated with the first to fifth mineralization stages with high extension of native gold particles, chalcopyrite, tennantite-tetrahedrite, galena and sphalerite mineralization especially for Z1, Z2 and Z3 (Shahbazi et al. 2019). They are correlated with silicification, intermediate argillic alteration and sericitization. Moreover, these veins are associated with faults and fractures and intrusive bodies specifically the microdiorite porphyry (Fig 6).

Geochemical populations obtained through multifractal modeling were correlated with mineralization phases derived via mineralographical and field geological data. Elemental anomalies especially enriched parts associate with faults and the microdiorite porphyry intrusive (Fig 7). High intensive gold mineralized Z1-Z3 veins occurred in the same directions of NW-SE and E-W (Figs 2, 3 and 5). Based on fractal modeling, intensive phase for gold mineralization commences from 7.94 ppm with the third geological phase including hematite mineralization within silicic veins and tuff andesitic rocks. Another main stage of gold mineralization contains Au concentrations between 2.24 and 7.94 ppm which is associated with sulfide Zn-Pb mineralization as sphalerite, galena, tetrahedrite, pyrite and gold inclusions in the sphalerite and galena. The FD for Au enriched zone is 1.77 which is highest value among FDs of the C-N log-log plot of the Au. Boiling is the major process for gold enrichment and also, weathering is an effective reason for secondary enriched mineralization (Sillitoe and Hedenquist, 2003). Multifractal nature of the log-log plots can be used for separation of these steps. Boiling process was carried out in Au values higher than 7.94 ppm (Fifrth population). In last hydrothermal activities, previous minerals have been brecciated and cemented by quartz- carbonate. This breccia phase contains 1.26- 2.24 ppm (third population). High porosity of tuff is a proper conduit for mineralization during hydrothermal ore-forming processes.

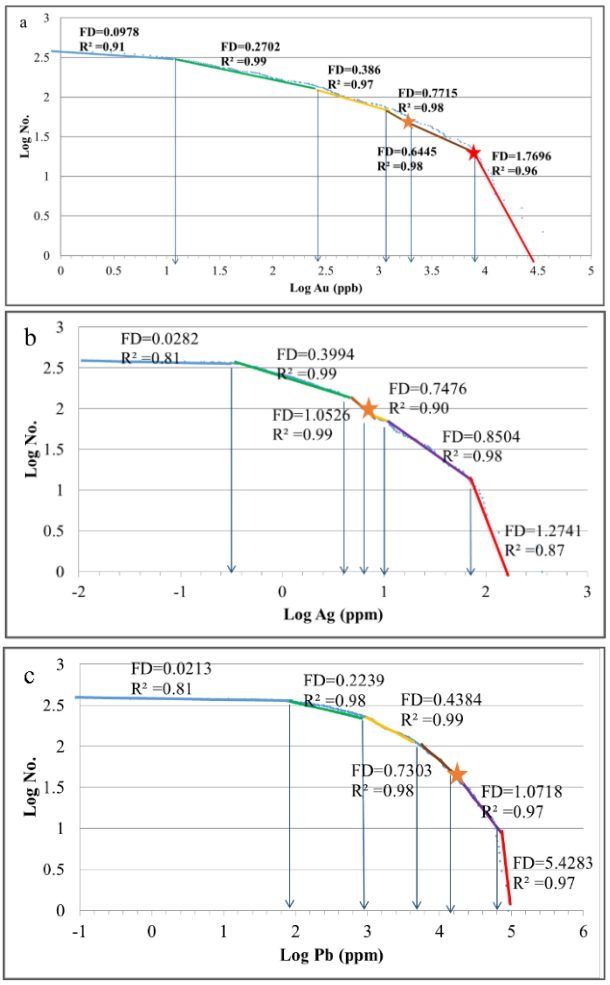

Fig 5. C-N log-log plots for different elements. FD: Fractal Dimension and R2 show accuracy of fitness for every populations. Orange stars indicate main mineralization commencing for study elements and red star reveals enriched zone for Au.

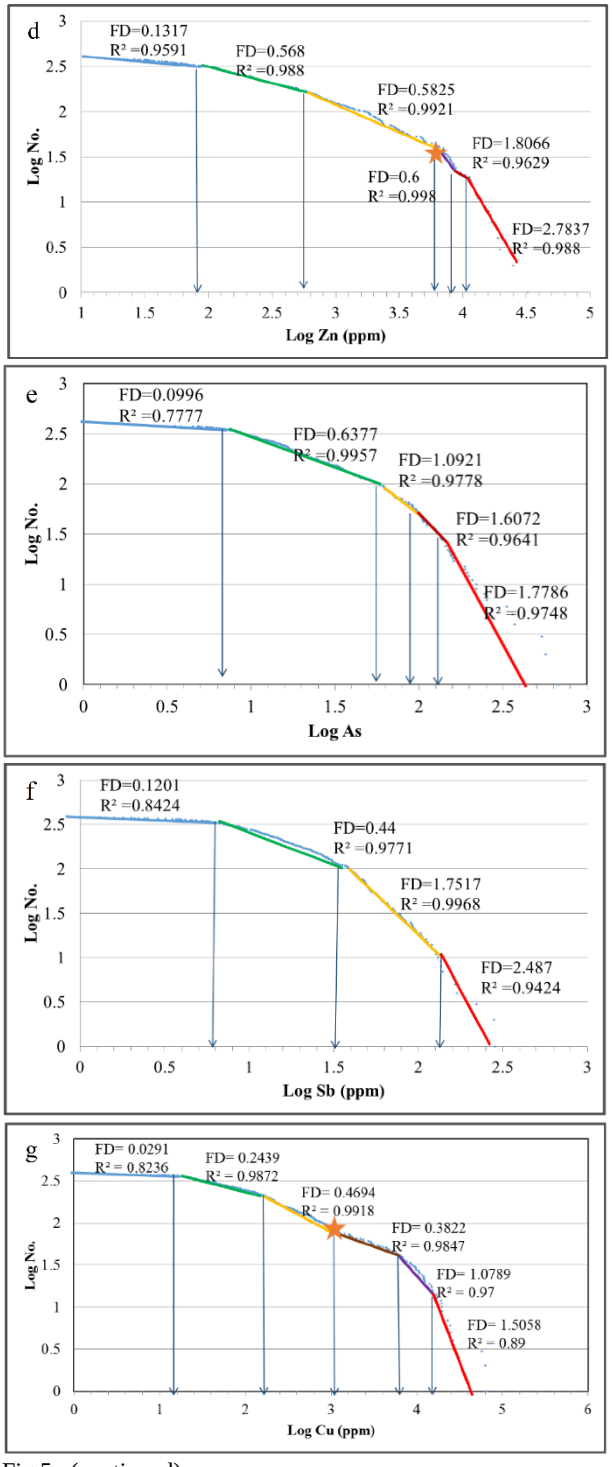

Fig 5. (continued).

High density of faults and fractures increased porosity of the host rocks especially the tuff andesitic rocks. A proximal intrusive body adjacent to the tuffs provided heat for the ore-forming fluids. Differences between populations of the C-N log-log plots for effective elements in the study ore deposit type can be used for better interpretation of ore-forming processes with correlation by geological characteristics (Fig 5).

Geochemical populations obtained through multifractal modeling were correlated with mineralization phases derived via mineralographical and field geological data. Elemental anomalies especially enriched parts associate with faults and the microdiorite porphyry intrusive (Fig 7). High intensive gold mineralized Z1-Z3 veins occurred in the same directions of NW-SE and E-W (Figs 2, 3 and 5). Based on fractal modeling, intensive phase for gold mineralization commences from 7.94 ppm with the third geological phase including hematite mineralization within silicic veins and tuff andesitic rocks. Another main stage of gold mineralization contains Au concentrations between 2.24 and 7.94 ppm which is associated with sulfide Zn-Pb mineralization as sphalerite, galena, tetrahedrite, pyrite and gold inclusions in the sphalerite and galena. The FD for Au enriched zone is 1.77 which is highest value among FDs of the C-N log-log plot of the Au. Boiling is the major process for gold enrichment and also, weathering is an effective reason for secondary enriched mineralization (Sillitoe and Hedenquist, 2003). Multifractal nature of the log-log plots can be used for separation of these steps. Boiling process was carried out in Au values higher than 7.94 ppm (Fifrth population). In last hydrothermal activities, previous minerals have been brecciated and cemented by quartz- carbonate. This breccia phase contains 1.26- 2.24 ppm (third population). High porosity of tuff is a proper conduit for mineralization during hydrothermal ore-forming processes. High density of faults and fractures increased porosity of the host rocks especially the tuff andesitic rocks. A proximal intrusive body adjacent to the tuffs provided heat for the ore-forming fluids. Differences between populations of the C-N log-log plots for effective elements in the study ore deposit type can be used for better interpretation of ore-forming processes with correlation by geological characteristics (Fig 5).

The results obtained by the C-N fractal model are compared with statistical analysis of data for Au. Based on the abnormal distribution of the gold (Fig 8), median (M: 80 ppb) and its summation with standard deviation (SD) used for separation of various anomalies and populations for gold (Davis 2002). Different Au populations were detected based on M, M+SD and M+2SD which equal to 80 ppb, 3.874 ppm and 7.668 ppm. The standard deviation is very high value (3794 ppm) which cause many gold populations dismissed, but the fractal methodology is distinguished many zones and phases in all parts of the gold concentrations' variations. Moreover, SDs for other elements are high and many zones were dismissed based on classical statistics. This phase consists of chalcopyrite, sphalerite and pyrite correlating with the second mineralization phase. Fractal dimension for the second stage for Au is 0.77. According to fractal modeling, the first gold mineralization stage includes Au values between 0.014 and 0.32 ppm with FD equal to 0.27. There are sulfidic gels with low contents of sphalerite, chalcopyrite and pyrite.

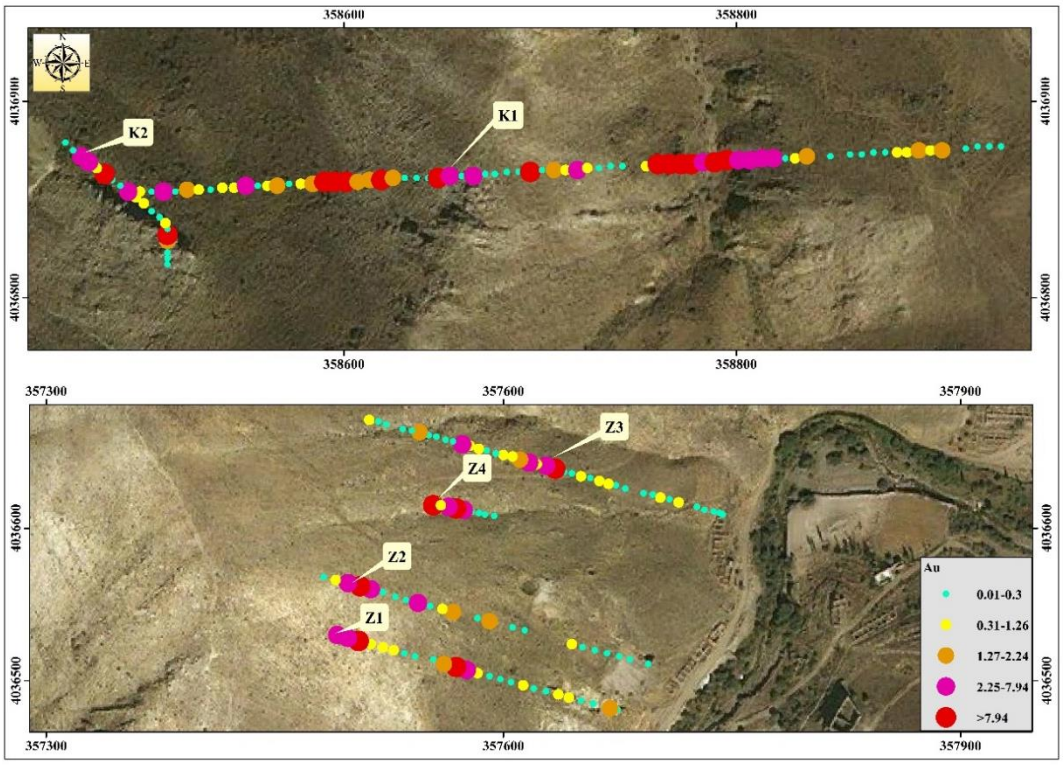

Fig 6. Au distribution in K1, K2, Z1, Z2, Z3 and Z4 veins based on the C-N fractal modeling

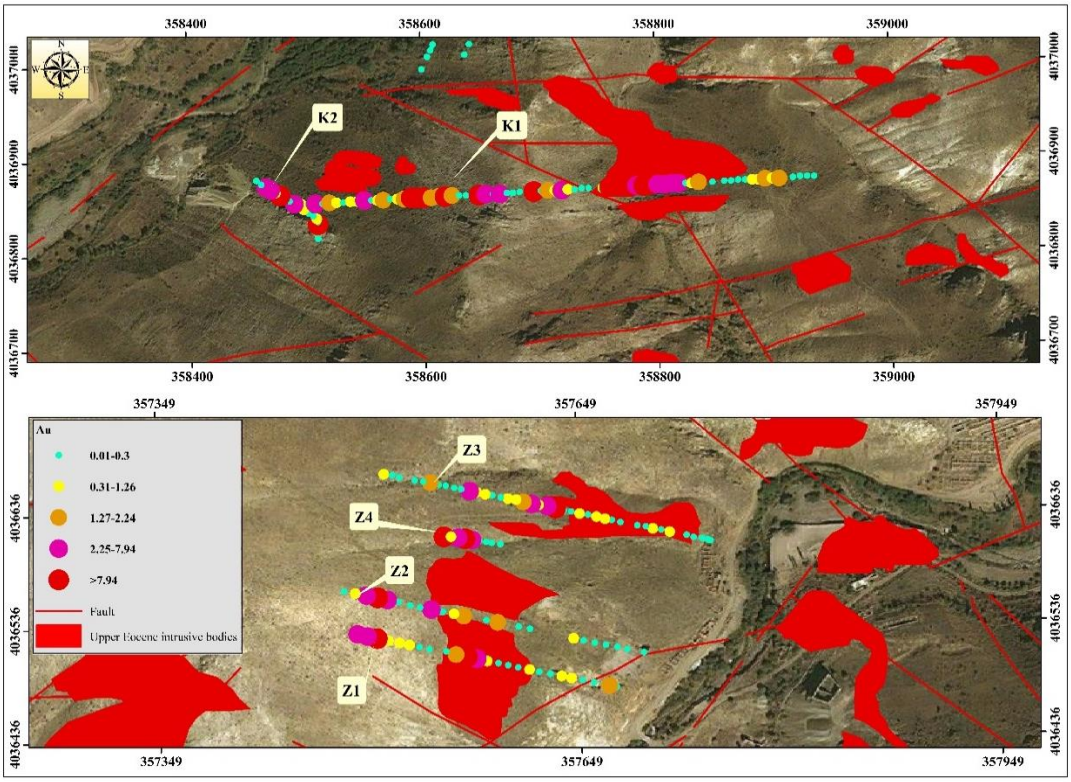

Fig 7. The relationship between intrusive bodies, faults and high intensive gold mineralized veins. A: in K1 and K2 veins. B: in Z1-Z4 veins.

Gold concentrations lower than 0.014 ppm are equal to gold values in the volcanic rocks as background (Cu≤0.2%) with FD lower than 0.1. The major population for silver contains Ag contents higher than 79.4 ppm which has good correlation with silicic veins in the faults. There are tetrahedrite and tennantite with high contents of silver. In addition, arsenic and antimony have concentrations higher than 141 ppm and 125.9 ppm, respectively, with Pb-Zn sulfide mineralization. Major Pb-Zn mineralization obtained by fractal modeling has Pb and Zn contents higher than 15.8% and 8.9% with FDs ≥ 1 and ≥ 0.6, respectively, which is related to high amount of galena and sphalerite occurrences (the forth geological phase; Fig 5). Other stage of Pb mineralization contains Pb and Zn contents of 6.3%-15.8% and 6.3%-8.9% with FD values equal to 0.73 and 0.58, respectively, represented by galena veinlets crosscutting the earlier mineralization and also, occurrence of sphalerite and chalcopyrite. The first population for Pb log-log plot has Pb and FD contents lower than 0.13% and 0.2, respectively, which is correlated with tuffs all of which related to faults, silicic veins and the microdioritic intrusive mass. Arsenic and antimony populations with concentrations of 63-100 ppm (FD=1.1) and 7.94-39.8 ppm (FD=0.44), respectively, are associated with major copper mineralization represented by chalcopyrite and bornite (Cu≥15.8% and FD=1.5). There is a direct relationship between mineralized phases and FD values for these elements (Table 1). In the enriched populations, FD values are increased more than 1. The FD for enriched zones for Pb, Zn and Sb are higher than 2 which is shown in Fig 5.

Table 1. Compare of geological signature with fractal results

	Background	Phase1	Phase2	Phase3	Phase4	Phase5
mineralogy		Pyrite-Chalcopyrite-Sphalerite	Pyrite-Chalcopyrite-Sphalerite	gold- Hematite	Pyrite-Chalcopyrite-Sphalerite- Galena- Tenantite-tetrahedrite- Gold	All of last sulfidic minerals
Alteration		Silisic	Silisic	Silisic	Silisic	Silisic- Carbonate
Geometry		Sulfidic Gels in Silisic patch	Breccia, Vein and veinlet	Vein and veinlet	Breccia, Vein and veinlet	Vein and breccia
Grade (Au)	<0.014	0.014-0.31	0.31-1.26	>7.94	2.24-7.94	1.26-2.24
Fractal Dimention (Au)	0.0978	0.2702	0.386	1.7696	0.6445	0.7715
R2 (Au)	0.91	0.99	0.97	0.96	0.98	0.98
Grade (Ag)	<0.45	0.45-5	5-7.94	7.94-12.6	> 79.4	12.6- 79.4
Fractal Dimention (Ag)	0.0282	0.3994	1.0526	0.7476	1.2741	0.8504
R2 (Ag)	0.81	0.99	0.99	0.9	0.98	0.87
Grade (Pb)	<125.9	125.9- 1259	1259- 6310		15849-63096 and > 63096	6310- 15849
Fractal Dimention (Pb)	0.0213	0.2239	0.4384		1.0718 and 5.4283	0.7303
R2 (Pb)	0.81	0.98	0.99		0.97 and 0.97	0.98
Grade (Zn)	<100	100- 631	6310- 8912.5		8912.5- 11220 and > 11220	631-6310
Fractal Dimention (Zn)	0.1317	0.568	1.8066		0.6 and 2.7837	0.5825
R2 (Zn)	0.9591	0.998	0.9629		0.998 and 0.988	0.9921
Grade (As)	< 7.94		63.09-100	7.94-63.09	>141	100-141
Fractal Dimention (As)	0.0996		1.0921	0.6377	1.7786	1.6072
R2 (As)	0.7777		0.9778	0.9957	0.9748	0.9641
Grade (Sb)	< 7.94		7.94-39.91		>125.9	39.91-125.9
Fractal Dimention (Sb)	0.1201		0.44		2.487	1.7517
R2 (Sb)	0.8224		0.9771		0.9424	0.9968
Grade (Cu)	<15.85	15.85-199.5	6309.6-15849 and >15849		1258.9-6309.6	199.5-1258.9
Fractal Dimention (Cu)	0.0291	0.2439	1.0789 and 1.5058		0.3822	0.4694
R2 (Cu)	0.8236	0.9872	0.97 and 0.89		0.9847	0.9918

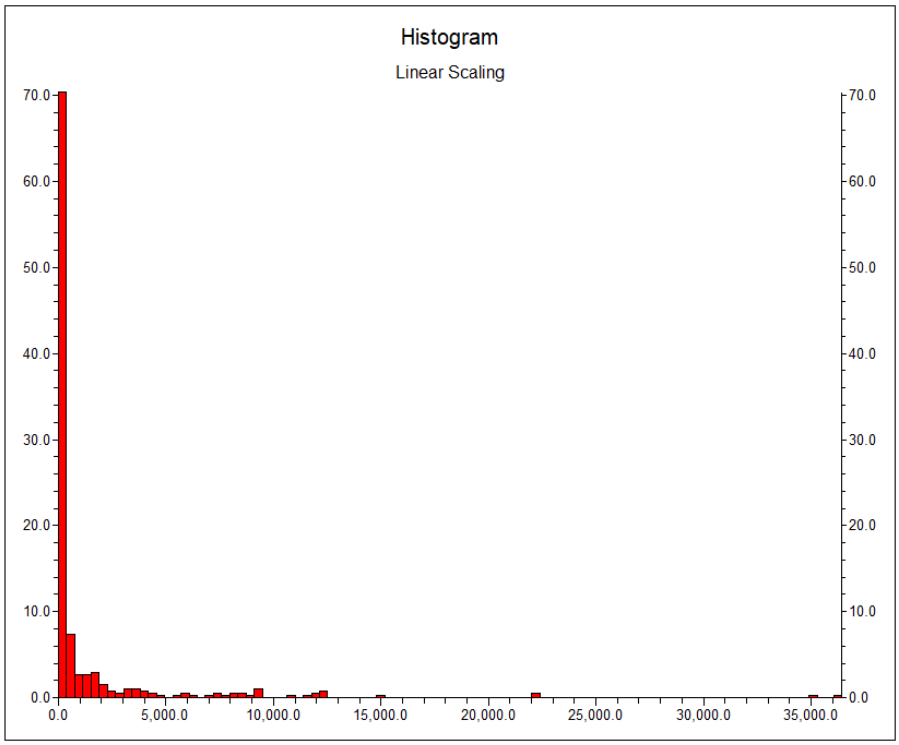

Fig 8. Au histogram which shows abnormal distribution.

6. Conclusions

Results obtained by the fractal modelling of various elements represent different mineralization phases for gold. A direct relationship between mineralized phases, ore grades and FD values exist for study elements. The FDs are increased more than 1 in the elemental enriched populations. The FD for enriched zones for Pb, Zn and Sb are higher than 2. Consequently, FDs are lower than 0.15 for background zones of the study elements. Mineralized veins at the Zehabad deposit occur within faults and structures due to the intrusion of microdioritic porphyry. Mineralization phases obtained through fractal modeling are compared with geological data. The first phase of mineralization of Au, Cu, Pb, Zn and Ag as sulfidic gels and silicic veins is a low intensive mineralization correlated with first population of fractal modelling including Au<0.014 ppm, Cu<16ppm, Ag<0.4 ppm, Pb<112 ppm and Zn< 100 ppm. The second phase contains chalcopyrite, sphalerite, pyrite and bornite with silicic veins. The highest copper grade is detected in this phase. Based on calcite blades, mineralization in the third phase happened due to boiling. The third mineralization phase consists of specular hematite and native gold particles. The fourth phase includes Au, Ag, Pb and Zn mineralization and low values of native copper within the silicic veins. However, the highest grades for As and Sb are recorded in this phase. Gold is increased as inclusions in galena and sphalerite while tetrahedrite provided Cu, As, Ag and Sb to the system. The fifth stage presents barren silicic veins which are resulted from the last pulses of ore-forming fluids.

Acknowledgments

This paper is part of the first author's Ph.D. thesis project at Tarbiat Modares University, Tehran, Iran. Executive manager of the Amin Khorramdasht Co. and Mr. Ali Baghi are thanked for their assistance in the study. The senior author would also like to acknowledge Samaneh Kansar Zamin Co. for its support.

References

Afzal P, Dadashzadeh Ahari H, Omran NR, Aliyari F (2013) Delineation of gold mineralized zones using concentration–volume fractal model in Qolqoleh gold deposit, NW Iran, *Ore Geology Reviews* 55: 125–133.

Afzal P, Khakzad A, Moarefvand P, Rashidnejad Omran N, Fadakar Alghalandis Y (2011) Delineation of mineralization zones in porphyry Cu deposits by fractal concentration–volume modeling, *Geochemical Exploration* 108: 220–232.

Aghazadeh M, Castro A, Badrzadeh Z, Vogt K, (2011) Post-collisional polycyclic plutonism from the Zagros hinterland. The Shaivar-Dagh plutonic complex Alborz belt, Iran. *Geol. Mag*. 148, 980–1008.

Agterberg FP, Cheng Q, Brown A, Good D (1996) Multifractal modeling of fractures in the Lac du Bonnet batholith, Manitoba, *Comput. Geosci* 22(5): 497–507.

Amin Khorramdasht Exploration Company (2006) Final Report of Technical Services in Zehabad Pb-Zn Deposit. *Internal Report*. Tehran, Iran: Amin Khorramdasht Exploration Company (in Persian).

Asiabanha A, Foden F (2012) Post-collisional transition from an extensional volcano-sedimentary basin to a

continental arc in the Alborz ranges, N-Iran. *Lithos* 148: 98-111.

Castro A, Aghazadeh M, Badrzadeh Z, Chichorro M (2013) Late Eocene–Oligocene post-collisional monzonitic intrusions from the Alborz magmatic belt, NW Iran. An example of monzonite magma generation from a metasomatized mantle source, *Lithos* 180-181: 109–127.

Cheng Q, Agterberg FP, Ballantyne SB (1994) The separartion of geochemical anomalies from background by fractal methods, *Geochemical Exploration* 51: 109–130.

Esmaeli M, Lotfi M, Nezafati N (2015) Fluid inclusion and stable isotope study of the Khalyfehlou copper deposit, southeast Zanjan, Iran, *Arabian Journal of Geoscience* 8 (11): 9625–9633.

Hassanpour S, Afzal P (2013) Application of concentration–number (C–N) multifractal modeling for geochemical anomaly separation in Haftcheshmeh porphyry system, NW Iran, *Arabian Journal of Geosciences* 6(3): 957–970.

Khalili H, Afzal P (2018) Application of spectrum-volume fractal modeling for detection of mineralized zones, *Journal of Mining & Environment* 9(2): 371–378.

Kouhestani H, Mokhtari MAA, Chang Z, Johnson CA (2018) Intermediate sulfidation type base metal mineralization at Aliabad-Khanchy, Tarom-Hashtjin metallogenic belt, NW Iran, *Ore Geology Reviews* 93: 512–521.

Li C, Ma T, Shi J (2003) Application of a fractal method relating concentrations and distances for separation of geochemical anomalies from background, *Geochemical Exploration* 77: 167–175.

Mandelbrot BB (1983) The fractal geometry of nature. *Freeman*, San Francisco.

Mehrabi B, Ghasemi M, Goldfarb R, Azizi H, Ganerod M, Marsh E (2016) Mineral assemblages, fluid evolution and genesis of polymetallic epithermal veins, Glojeh district, NW Iran, *Ore Geology Reviews* 78: 41–57.

Mokhtari MAA, Kouhestani H, Pang KN, Chung SL (2018) Age and geochemical constraints on granitoid petrogenesis in the Khorram Darag-Khakriz region (36.5˚N, 48.5˚E), Urumieh-Dokhtar magmatic arc, NW Iran, *Geochemistry Symposium*, Antalya, Turkey.

Nabatian G, Ghaderi M (2014) Mineralogy and geochemistry of rare earth elements in iron oxide - apatite deposits of the Zanjan region, *Scientific Quarterly Journal of Geosciences* 24(93): 157–170.

Nabatian G, Ghaderi M, Corfu F, Honarmand M (2014) Geology, alteration, age, and origin of iron oxide–apatite deposits in Upper Eocene quartz monzonite, Zanjan district, NW Iran, *Mineralium Deposita* 49(2): 217–234.

Nabatian G, Wan B, Honarmand M (2017) Whole rock geochemistry, molybdenite Re-Os geochronology, stable isotope and fluid inclusion investigations of the Siah-Kamar deposit, western Alborz-Azarbayjan: New constrains on the porphyry Mo deposit in Iran, *Ore Geology Reviews* 91:638-659.

Nabavi MH (1976) Introduction to Geology of Iran. Tehran, Iran, Geological Survey of Iran.

Rezaeian M, Carter A, Hovius N, Allen M B (2012) Cenozoic exhumation history of the Alborz Mountains, Iran: New constraints from low-temperature chronometry, *Tectonics*, 31, TC2004.

Sim BL, Agterberg FP, Beaudry C (1999) Determining the cutoff between background and relative base metal contamination levels using multifractal methods, *Comput. Geosci* 25: 1023–1041.

Shahbazi S (2020) Geochemistry and genesis of Zehabad Pb-Zn-Au-Ag-Cu polymetallic deposit in NW Iran, *P.hd thesis, Tarbiat Modares university*, Iran.

Shahbazi S, Ghaderi M (2014) Zehabad gold mineralization: an example of epithermal deposits related to high-potassium magmatism in post-subduction extension environment, *18th Symposium of the Geological Society of Iran*: 4.

Shahbazi S, Ghaderi M, Alfonso P (2019) Mineralogy, alteration, and sulfur isotope geochemistry of the Zehabad intermediate-sulfidation epithermal deposit, NW Iran, *Turkish Journal of Earth Sciences* 28(6): 882-901.

Shahbazi S, Ghaderi, M, Madanipour S (2018) The role of Zanjan-Manjil semi-brittle zone in controlling the Zehabad Pb, Zn, Au, Ag (Cu) mineralization, NW Qazvin, *The 36th National and the 3rd National Geosciences Congress*, Tehran, Iran.

Yasami N, Ghaderi, M, Alfonso P (2018) Sulfur isotope geochemistry of the Chodarchay Cu-Au deposit, Tarom, NW Iran, *Neues Jahrbuch für Mineralogie - Abhandlungen* 195(2): 101–113.